MedChemComm

Accepted Manuscript

ROYAL SOCIETY OF CHEMISTRY

www.rsc.org/medchemcomm

Table of Contents (TOC) Image

Multifunctional dendrimers modified with alpha-tocopheryl succinate for targeted cancer therapy†

Yun Zheng,[ab1] Fanfan Fu,[b1] Mengen Zhang,[a] Mingwu Shen,*[a] Meifang Zhu,[b] Xiangyang Shi*[ab]

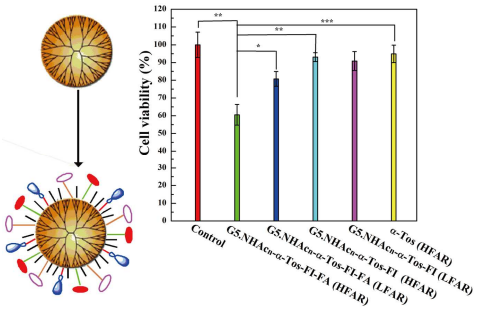

Multifunctional generation 5 poly(amidoamine) dendrimers can be used as a platform to covalently conjugate alpha-tocopheryl succinate for targeted cancer therapy.

MedChemComm

Cite this: DOI: 10.1039/c0xx00000x

www.rsc.org/xxxxxx

CONCISE ARTICLE

Multifunctional dendrimers modified with alpha-tocopheryl succinate for targeted cancer therapy†

Yun Zheng,[ab1] Fanfan Fu,[b1] Mengen Zhang,[a] Mingwu Shen,*[a] Meifang Zhu,[b] Xiangyang Shi*[ab]

Received (in XXX, XXX) Xth XXXXXXXXX 20XX, Accepted Xth XXXXXXXXX 20XX

DOI: 10.1039/b000000x

Generation 5 poly(amidoamine) dendrimers were used as a nanoplatform to covalently conjugate an anticancer drug alpha-tocopheryl succinate (α-Tos) and targeting ligand folic acid (FA). The formed multifunctional dendrimers are able to endow the hydrophobic drug α-Tos with improved water solubility for targeted inhibition of cancer cells via FA receptor-mediated targeting pathway.

Conventional anticancer chemotherapeutic agents suffer a general problem of non-specific distribution in the body, thereby exerting side-effect on the normal tissues.[1, 2] Moreover, numerous cancer drugs lack water solubility and bioavailability, substantially limiting their applications in cancer therapy. Therefore, it is essential to develop various nanocarrier systems to overcome these hurdles.[3, 4] Among the many studied nanocarrier systems, in particular nanoparticle-based drug delivery systems,[5-7] dendrimers have received a great deal of attention due to their unique structural characteristics such as monodispersity, high density of peripheral functional groups, well-defined globular shape, multivalency, and nonimmunogenecity.[8-10] One of the major advantages to use dendrimers as a carrier system is that the size of dendrimers is quite small (e.g., the diameter of a generation 5 (G5) poly(amidoamine) (PAMAM) dendrimer is 5.4 nm), which enables them to be easily cleared from the blood through kidney,[11] eliminating the need for biodegradability.

The use of dendrimers, especially PAMAM dendrimers as drug carriers have been proven to be versatile.[12-18] PAMAM dendrimers can be used either to physically encapsulate hydrophobic drugs within the highly branched internal cavity or as a platform to covalently conjugate drug molecules onto their surface for drug delivery applications.[18-21] In addition, the well-defined surface functional groups of dendrimers enable the facile modification of various targeting moieties and imaging agents onto the dendrimers for imaging-guided targeted drug delivery applications.[22-26] For instance, G5 PAMAM dendrimers have been used as a unique platform to covalently conjugate targeting ligand folic acid (FA), imaging dye fluorescein isothiocyanate (FI), and cancer drug methotrexate for simultaneous targeting, imaging, and treatment of cancer.[17, 27-29] In our previous work, we have shown that acetamide-terminated G5 PAMAM dendrimers modified with FA and FI are able to physically encapsulate different cancer drugs (2-methoxyestradiol, doxorubicin, or combretastatin A4) for targeted delivery to cancer cells overexpressing FA receptors (FAR).[30-32] These studies clearly suggest that dendrimers are indeed a unique platform that can be used for targeted delivery of cancer drugs via either physical encapsulation or covalent conjugation of drug molecules.

Alpha-tocopheryl succinate (α-Tos), also known as vitamin E succinate, is a well-known derivative of vitamin E that constitutes three domains: the functional domain, the signaling domain, and the hydrophobic domain.[33-35] α-Tos has been reported to have anticancer activity against a wide range of human cancer cells[36] through induction of apoptosis, cell cycle blockage, and disruption of the necessary autocrine signaling pathways of tumor growth.[37-45] Importantly, α-Tos has been reported to be non-toxic to normal cells.[46, 47] However, the conventional formulation of α-Tos dissolved in ethanolic solution significantly limits its biomedical applications owing to the lack of water solubility and bioavailability. It is essential to develop a nanoscale delivery system that is able to improve the water solubility and bioavailability of α-Tos. Recent work reported by Kim et al.[48] has shown that recombinant human gelatin conjugated with lipoic acid is able to form nanoparticles (NPs) in aqueous solution and encapsulate α-Tos during the self-assembly process for delivery of α-Tos to cancer cells via the known passive enhanced permeability and retention (EPR) effect. In another work,[49] Dou and coworkers reported that α-Tos-conjugated chitosan oligosaccharide NPs were able to physically load paclitaxel for synergistic chemotherapy. Most of the studies related to delivery of α-Tos have not been involved in the modification of the NPs with active targeting ligands. With the prior advances of dendrimer nanotechnology, we hypothesize that α-Tos may be covalently linked onto the surface of PAMAM dendrimer, followed by modification of the dendrimer terminal amines with acetamide, imaging dyes, and targeting ligands for targeted delivery of α-Tos to cancer cells.

To prove our hypothesis, in this present study, we utilized G5 PAMAM dendrimers as a platform to sequentially conjugate α-Tos, imaging dye FI, and targeting ligand FA for

targeted cancer therapy applications. In our work, G5 PAMAM dendrimers were first covalently linked with α-Tos via an amide bond, and then a majority of dendrimer terminal amines were acetylated. After that, the remaining dendrimer terminal amines were covalently conjugated with FI and FA (Scheme 1). The formed dendrimer conjugates were characterized by ^{1}H NMR and UV-Vis spectroscopy. The anticancer activity of the dendrimer conjugates and their performance in targeted cancer cell inhibition were evaluated by 3-[4,5-dimethyl-2-thiazolyl]-2,5-diphenyl-2H-tetrazolium bromide (MTT) cell viability assay. The cancer cell targeting efficiency was investigated by flow cytometry and confocal microscopy. To our knowledge, this is the first report related to the development of α-Tos delivery system using dendrimer-based nanotechnology.

Previous work has shown that by conjugating α-Tos with water-soluble and biodegradable polymers via an amide bond, the water solubility of α-Tos can be significantly improved and the therapeutic efficacy of α-Tos is not compromised.[35, 49] Owing to the advantages of dendrimer carrier system, we chose to conjugate α-Tos onto the surface of G5.NH_2 dendrimer to develop a multifunctional drug delivery system (G5.$NHAc_n$-α-Tos-FI-FA conjugate) for targeted cancer therapy.

The multifunctional G5.$NHAc_n$-α-Tos-FI-FA conjugate was synthesized in four steps (Scheme 1). Firstly, G5.NH_2 dendrimer was covalently linked with α-Tos (with 10 α-Tos linked onto each dendrimer) via an amide bond via a 1-(3-dimethylaminopropyl)-3-ethylcarbodiimide hydrochloride (EDC) coupling reaction between the dendrimer terminal amines and the carboxyl groups of α-Tos. Secondly, to enhance the biocompatibility of the dendrimer conjugate, a large portion of dendrimer terminal amines on the G5 dendrimer surface were acetylated to minimize the nonspecific binding of the dendrimers with negatively charged cell membranes. Thirdly, to detect the intracellular uptake of the dendrimer conjugate, 6 FI moieties were covalently conjugated onto each G5.$NHAc_n$-α-Tos conjugate by reacting with the remaining dendrimer terminal amines according to our previous studies.[30-32] At last, 8 molar-equivalent FA, which is known to be sufficient to target cancer cells overexpressing high-affinity FAR with high efficiency,[50] were linked onto each G5.$NHAc_n$-α-Tos-FI dendrimer via an amide bond between the γ-carboxyl group of FA and the remaining dendrimer terminal amines. Note that the numbers of 10, 6, and 8 are associated with the molar feeding ratios of 10:1, 6:1, and 8:1 between the respective small molecules and the G5 dendrimer.

The chemical structure of the formed G5.$NHAc_n$-α-Tos-FI-FA conjugate was characterized by ^{1}H NMR (Figure 1). The peak at 1.87 ppm can be assigned to the -CH_3 protons of the acetyl groups, while the peak at 0.75 ppm is associated with the -CH_3 protons of α-Tos. In addition, the peaks in the aromatic proton region are attributed to the characteristic proton peaks from FI (peaks a, b, and c) and FA (peaks d, e, and f), in agreement with our previous work.[32] By appropriate NMR integration, the average number of α-Tos, acetyl group, FI, and FA coupled to each dendrimer was estimated to be 5.0, 85.0, 4.5, and 5.3, respectively. The chemical structures of the G5.$NHAc_n$-FI-FA dendrimer without α-Tos conjugation and the G5.$NHAc_n$-α-Tos-FI conjugate without FA were also synthesized under similar conditions described in Scheme 1. The two dendrimer products were characterized by ^{1}H NMR (Figures S1 and S2, Electronic Supplementary Information, ESI) and used to compare with the G5.$NHAc_n$-α-Tos-FI-FA conjugate in biological applications.

The G5.$NHAc_n$-α-Tos-FI-FA conjugate was then characterized by UV-Vis spectroscopy (Figure 2). UV-Vis spectra of G5.NH_2, G5.NH_2-α-Tos, G5.$NHAc_n$-α-Tos, and G5.$NHAc_n$-α-Tos-FI dendrimers are also given for comparison. It can be seen that G5.NH_2 does not show any significant absorption above 250 nm due to its aliphatic structural nature. After conjugating with α-Tos, both G5.NH_2-α-Tos and G5.$NHAc_n$-α-Tos dendrimers have an absorption peak at 283 nm, indicating the successful modification of G5 dendrimer with α-Tos. Further modification of FI onto the G5.$NHAc_n$-α-Tos dendrimer gives rise to a prominent absorption peak at 500 nm, which is associated with the typical FI absorption. Furthermore, the final modification of FA ligands results in a featured absorption peak of FA at 280 nm for the G5.$NHAc_n$-α-Tos-FI-FA conjugate. Both ^{1}H NMR and UV-Vis spectroscopy data suggest the successful synthesis of multifunctional G5.$NHAc_n$-α-Tos-FI-FA conjugate.

The stability of the G5.$NHAc_n$-α-Tos-FI-FA conjugate is crucial for their biological applications. Similar to the G5.$NHAc_n$-FI-FA dendrimers without α-Tos synthesized according to our previous work with slight modification,[32] we show that the lyophilized G5.$NHAc_n$-α-Tos-FI-FA conjugate is able to be completely dissolved in aqueous solution, and is stable under different pH conditions (pH 5.0, 7.0, 10.0) for at least 2 months (Figure S3, ESI). Table 1 shows the surface potentials of G5.$NHAc_n$-FI-FA and G5.$NHAc_n$-α-Tos-FI-FA conjugates under different pH conditions. The larger surface potential values at pH 5.0 than those at pH 7.0 for both dendrimers should be attributed to the pronation of a portion of the dendrimer tertiary amines.[51] The variation of the surface potential of both dendrimers with pH followed the same trend to that of G5.NHAc dendrimers as described in our previous work.[21] In addition, the G5.$NHAc_n$-α-Tos-FI-FA conjugate dispersed in different aqueous media (e.g., water, phosphorate buffered saline (PBS), and cell culture medium) stored in 4 ℃ were stable for at least 6 months (Figure S4, ESI), which is essential for their further biomedical applications. Furthermore, the conjugate was exposed to PBS at room temperature for at least one month, no free drug release was detected.

KB cells, a human epithelial carcinoma cell line, were used to test the therapeutic efficacy of G5.$NHAc_n$-α-Tos-FI-FA conjugate. MTT assay was performed to test the viability of KB cells treated with the conjugate for 48 h (Figure 3). Free α-Tos and non-targeted G5.$NHAc_n$-α-Tos-FI conjugate were also tested for comparison. It can be seen that free α-Tos starts to exert a therapeutic effect to KB cells at a concentration of 100 μM, while the G5.$NHAc_n$-α-Tos-FI-FA conjugate is able to inhibit the growth of KB cells at α-Tos concentration of 25

μM. Likewise, compared to the targeted G5.NHAc$_n$-α-Tos-FI-FA conjugate, the non-targeted G5.NHAc$_n$-α-Tos-FI conjugate displays less cytotoxicity at the α-Tos concentration above 50 μM ($p < 0.05$), suggesting that the targeted G5.NHAc$_n$-α-Tos-FI-FA conjugate may have a better cellular uptake *via* ligand-receptor interaction. Our data suggest that the G5.NHAc$_n$-α-Tos-FI-FA conjugate has a better therapeutic efficacy than free α-Tos, possibly due to the fact that the dendrimer conjugate is able to be easily uptaken by the cells. We also show that the viability of KB cells treated with PBS (10 μL) used to dissolve the dendrimer species, ethanol solvent (1 μL) used to dissolve free α-Tos, and G5.NHAc$_n$-FI-FA dendrimer in PBS (10 μL) with concentrations corresponding to those of the conjugate (at different α-Tos concentrations) does not have any appreciable changes when compared to the control KB cells without treatment. This suggests that the growth inhibition of KB cells is solely associated with the α-Tos drug, and the dendrimer carrier itself in the given concentration range and the used ethanol solvent do not have any appreciable effect on the cell viability.

To confirm the therapeutic efficacy of the G5.NHAc$_n$-α-Tos-FI-FA conjugate, the morphology of KB cells treated with the conjugate for 48 h was visualized (Figure S5, ESI). It is clear that KB cells treated with 1 μL ethanol (Figure S5b), 10 μL PBS (Figure S5d), and G5.NHAc$_n$-FI-FA dendrimer in 10 μL PBS (with concentration corresponding to that of the conjugate at α-Tos concentration of 50 μM, Figure S5e) display similar morphology to that of the control group without treatment (Figure S5a), indicating that the added ethanol, PBS, and G5.NHAc$_n$-FI-FA dendrimer are non-cytotoxic. In sharp contrast, a significant portion of KB cells treated with the G5.NHAc$_n$-α-Tos-FI-FA conjugate (Figure S5f) or free α-Tos (Figure S5c) with a drug concentration of 50 μM became rounded in shape, indicating that cells have undergone apoptosis. These results corroborate the MTT assay data. Our results clearly suggest that the conjugation of α-Tos on the surface of G5 dendrimer via an amide bond does not compromise the therapeutic efficacy of the drug, in agreement with the literature.[49]

FA was selected as a targeting ligand to be covalently conjugated onto the dendrimer surface in order to achieve targeted delivery of the α-Tos drug to cancer cells overexpressing high-affinity FAR, which is known to be overexpressed in many types of cancer cells, including the ovary, lung, breast, kidney, brain, endometrium, colon, and hematopoietic cells of myelogenous origin.[52] To confirm the targeting specificity of the G5.NHAc$_n$-α-Tos-FI-FA conjugate, KB cells with both high level and low level of FAR expression (KB-HFAR and KB-LFAR) were incubated with the conjugates (G5.NHAc$_n$-α-Tos-FI-FA and G5.NHAc$_n$-α-Tos-FI) for 3 h and were observed via confocal microscopy (Figure 4). It is clear that only KB-HFAR cells treated with G5.NHAc$_n$-α-Tos-FI-FA conjugate display significant green fluorescence signal in the cytoplasm of the cells, which is associated with the conjugated FI. In contrast, KB-HFAR cells treated with G5.NHAc$_n$-α-Tos-FI conjugate without FA and KB-LFAR cells treated with either G5.NHAc$_n$-α-Tos-FI or G5.NHAc$_n$-α-Tos-FI-FA conjugates do not have the associated green fluorescence signal, which is similar to the control KB cells treated with PBS. Our results reveal that the developed G5.NHAc$_n$-α-Tos-FI-FA conjugate is able to specifically target to the KB-HFAR cells via a receptor-mediated manner, and the conjugation of the α-Tos onto the G5 dendrimer platform does not compromise the FA-mediated targeting specificity, in agreement with our previous results.[30, 31]

The targeting specificity of the G5.NHAc$_n$-α-Tos-FI-FA conjugate was further quantitatively confirmed by flow cytometric analysis of KB cells treated with the conjugate for 1 h (Figure S6, ESI). It can be seen that only KB-HFAR cells treated with G5.NHAc$_n$-α-Tos-FI-FA conjugate have a significant increase in green fluorescence signal. In contrast, the same KB-HFAR cells treated with FA-free G5.NHAc$_n$-α-Tos-FI conjugate, KB-LFAR cells treated with either G5.NHAc$_n$-α-Tos-FI or G5.NHAc$_n$-α-Tos-FI-FA conjugate do not display the same level of green fluorescence signal. These results suggest that the binding of G5.NHAc$_n$-α-Tos-FI-FA conjugate is quite specific to KB-HFAR cells, in agreement with the confocal imaging data.

To assess the targeted therapeutic efficacy of the G5.NHAc$_n$-α-Tos-FI-FA conjugate, after 3 h incubation of the G5.NHAc$_n$-α-Tos-FI-FA and G5.NHAc$_n$-α-Tos-FI conjugates with KB cells, the medium in wells was replaced with fresh medium and the cells were incubated for additional 48 h before MTT assay (Figure 5). It can be seen that the treatment of KB-HFAR cells with G5.NHAc$_n$-α-Tos-FI-FA conjugate results in a significant decrease of cell viability (about 60.5%, $p < 0.05$ versus control). In contrast, after treatment with G5.NHAc$_n$-α-Tos-FI conjugate, around 93% of KB-HFAR cells are still alive ($p > 0.05$ versus control). This suggests that the FA modification enables effective targeting of G5.NHAc$_n$-α-Tos-FI-FA conjugate to KB-HFAR cells via a receptor-mediated manner, thereby exerting the targeted therapeutic efficacy to inhibit the growth of KB-HFAR cells. Moreover, KB-LFAR cells treated with either G5.NHAc$_n$-α-Tos-FI-FA or G5.NHAc$_n$-α-Tos-FI conjugates are still viable when compared with the control KB-HFAR cells treated with PBS. These results clearly indicate that the G5.NHAc$_n$-α-Tos-FI-FA conjugate can target the FAR-overexpressing cancer cells and specifically inhibit the growth of cancer cells via receptor-mediated binding and intracellular uptake. It should be noted that the control of free α-Tos at 50 μM under similar experimental conditions does not exert any therapeutic effect to the cells, suggesting the difficulty of the cellular uptake of the free drug within 3 h.

In summary, we developed an effective new formulation of anticancer drug α-Tos by covalently conjugating the hydrophobic α-Tos onto a dendrimer platform for targeted cancer therapy. The formed multifunctional G5.NHAc$_n$-α-Tos-FI-FA conjugate is water-soluble and stable at different pH conditions and different aqueous media. We show that the conjugate is able to inhibit the growth of cancer cells, with a therapeutic efficacy better than the free α-Tos drug under similar experimental conditions. Importantly, the formed G5.NHAc$_n$-α-Tos-FI-FA conjugate can specifically target to cancer cells with high-level FAR expression via a receptor-

mediated endocytosis pathway and exhibit specific therapeutic efficacy to the targeted cancer cells. With the versatile dendrimer nanotechnology, different hydrophobic anticancer drugs may be covalently conjugate onto dendrimer platforms to form multifunctional drug conjugates modified with different targeting ligands, thereby providing many possibilities for targeted cancer therapeutic applications.

This research is financially supported by the Fund of the Science and Technology Commission of Shanghai Municipality (12520705500 for M. S. and 11nm0506400 for X. S.), National Natural Science Foundation of China (81101150 and 21273032), the High-Tech Research and Development Program of China (2012AA030309), the Program for New Century Excellent Talents in University, State Education Ministry, and the Program for Professor of Special Appointment (Eastern Scholar) at Shanghai Institutions of Higher Learning. X. S. gratefully acknowledges and the Science and Technology Collaboration Fund between China and Hungary, Ministry of Science and Technology.

Notes and references

[a] *State Key Laboratory for Modification of Chemical Fibers and Polymer Materials, College of Materials Science and Engineering, Donghua University, Shanghai 201620, People's Republic of China*
[b] *College of Chemistry, Chemical Engineering and Biotechnology, Donghua University, Shanghai 201620, People's Republic of China. E-mail: xshi@dhu.edu.cn (X. Shi) or mingwu_shen@yahoo.com (M. Shen)*
[1] *These authors equally contributed to this work.*

† Electronic Supplementary Information (ESI) available: Experimental procedures and additional experimental results. See DOI: 10.1039/b000000x/

1. F. Danhier, O. Feron and V. Préat, *J. Control. Release*, 2010, **148**, 135-146.
2. M. A. Phillips, M. L. Gran and N. A. Peppas, *Nano Today*, 2010, **5**, 143-159.
3. L. Brannon-Peppas and J. O. Blanchette, *Adv. Drug Deliv. Rev.*, 2004, **56**, 1649-1659.
4. H. Maeda, G. Y. Bharate and J. Daruwalla, *Eur. J. Pharm. Biopharm.*, 2009, **71**, 409-419.
5. R. T. Chacko, J. Ventura, J. Zhuang and S. Thayumanavan, *Adv. Drug Deliv. Rev.*, 2012, **64**, 836-851.
6. T. Patel, J. Zhou, J. M. Piepmeier and W. M. Saltzman, *Adv. Drug Deliv. Rev.*, 2012, **64**, 701-705.
7. D. Peer, J. M. Karp, S. Hong, O. C. Farokhzad, R. Margalit and R. Langer, *Nat. Nanotechnol.*, 2007, **2**, 751-760.
8. M. Liu and J. M. J. Fréchet, *Drug Discov. Today*, 1999, **2**, 393-401.
9. T. Sakthivel and A. Florence, *Drug Deliv. Technol.*, 2003, **3**, 52-56.
10. S. H. Medina and M. E. H. El-Sayed, *Chem. Rev.*, 2009, **109**, 3141-3157.
11. D. Peer, J. M. Karp, S. Hong, O. C. FarokHzad, R. Margalit and R. Langer, *Nat. Nanotechnol.*, 2007, **2**, 751-760.
12. D. Tomalia, H. Baker, J. Dewald, M. Hall, G. Kallos, S. Martin, J. Roeck, J. Ryder and P. Smith, *Polym. J.*, 1985, **17**, 117-132.
13. R. Esfand and D. A. Tomalia, *Drug Discov. Today*, 2001, **6**, 427-436.
14. A. K. Patri, I. J. Majoros and J. R. Baker, Jr., *Curr. Opin. Chem. Biol.*, 2002, **6**, 466-471.
15. S. E. Stiriba, H. Frey and R. Haag, *Angew. Chem.-Int. Edit.*, 2002, **41**, 1329-1334.
16. I. J. Majoros, C. B. Mehta and J. R. Baker, Jr., *J. Comput. Theor. Nanosci.*, 2004, **1**, 193-198.
17. T. P. Thomas, I. J. Majoros, A. Kotlyar, J. F. Kukowska-Latallo, A. Bielinska, A. Myc and J. R. Baker, Jr., *J. Med. Chem.*, 2005, **48**, 3729-3735.
18. J. Zhu and X. Shi, *J. Mater. Chem. B*, 2013, **1**, 4199-4211.
19. R. Guo and X. Shi, *Curr. Drug Metab.*, 2012, **13**, 1097-1109.
20. M. T. Morgan, Y. Nakanishi, D. J. Kroll, A. P. Griset, M. A. Carnahan, M. Wathier, N. H. Oberlies, G. Manikumar, M. C. Wani and M. W. Grinstaff, *Cancer Res.*, 2006, **66**, 11913-11921.
21. X. Shi, I. Lee, X. Chen, M. Shen, S. Xiao, M. Zhu, J. R. Baker, Jr. and S. H. Wang, *Soft Matter*, 2010, **6**, 2539-2545.
22. R. Guo, Y. Yao, G. Cheng, S. H. Wang, Y. Li, M. Shen, Y. Zhang, J. R. Baker, Jr., J. Wang and X. Shi, *RSC Adv.*, 2012, **2**, 99-102.
23. T. P. Thomas, R. Shukla, A. Kotlyar, B. Liang, J. Y. Ye, T. B. Norris and J. R. Baker, Jr., *Biomacromolecules*, 2008, **9**, 603-609.
24. R. Shukla, T. P. Thomas, J. Peters, A. Kotlyar, A. Myc and J. R. Baker, Jr., *Chem. Commun.*, 2005, 5739-5741.
25. L. Zheng, J. Zhu, M. Shen, X. Chen, J. R. Baker, Jr., S. H. Wang, G. Zhang and X. Shi, *Med. Chem. Commun.*, 2013, **4**, 1001-1005.
26. T. P. Thomas, B. Huang, S. K. Choi, J. E. Silpe, A. Kotlyar, A. M. Desai, H. Zong, J. Gam, M. Joice and J. R. Baker, Jr., *Mol. Pharmaceutics*, 2012, **9**, 2669-2676.
27. I. J. Majoros, A. Myc, T. Thomas, C. B. Mehta and J. R. Baker, Jr., *Biomacromolecules*, 2006, **7**, 572-579.
28. I. J. Majoros, T. P. Thomas, C. B. Mehta and J. R. Baker, Jr., *J. Med. Chem.*, 2005, **48**, 5892-5899.
29. J. F. Kukowska-Latallo, K. A. Candido, Z. Cao, S. S. Nigavekar, I. J. Majoros, T. P. Thomas, L. P. Balogh, M. K. Khan and J. R. Baker, Jr., *Cancer Res.*, 2005, **65**, 5317-5324.
30. Y. Wang, X. Cao, R. Guo, M. Shen, M. Zhang, M. Zhu and X. Shi, *Polym. Chem.*, 2011, **2**, 1754-1760.
31. Y. Wang, R. Guo, X. Cao, M. Shen and X. Shi, *Biomaterials*, 2011, **32**, 3322-3329.
32. M. Zhang, R. Guo, Y. Wang, X. Cao, M. Shen and X. Shi, *Int. J. Nanomed.*, 2011, **6**, 2337.
33. M. Birringer, J. H. EyTina, B. A. Salvatore and J. Neuzil, *Br. J. Cancer*, 2003, **88**, 1948-1955.
34. J. Neuzil, *Br. J. Cancer*, 2003, **89**, 1822-1826.
35. Y.-W. Won, S.-M. Yoon, C. H. Sonn, K.-M. Lee and Y.-H. Kim, *ACS Nano*, 2011, **5**, 3839-3848.
36. K. N. Prasad, B. Kumar, X. D. Yan, A. J. Hanson and W. C. Cole, *J. Am. Coll. Nutr.*, 2003, **22**, 108-117.
37. K. Kline, G. S. Cochran and B. G. Sanders, *Nutr. Cancer*, 1990, **14**, 27-41.
38. K. N. Prasad, R. J. Cohrs and O. K. Sharma, *Biochem. Cell Biol.*, 1990, **68**, 1250-1255.
39. R. J. Cohrs, S. Torelli, K. N. Prasad, J. Edwards-Prasad and O. K. Sharma, *Int. J. Dev. Neurosci.*, 1991, **9**, 187-194.
40. J. Schwartz and G. Shklar, *J. Oral Maxillofac. Surg.*, 1992, **50**, 367-373.
41. J. M. Turley, B. G. Sanders and K. Kline, *Nutr. Cancer*, 1992, **18**, 201-213.

42. K. Israel, B. G. Sanders and K. Kline, *Nutr. Cancer*, 1995, **24**, 161-169.
43. M. Simmons‐Menchaca, M. Qian, W. Yu, B. G. Sanders and K. Kline, *Nutr. Cancer*, 1995, **24**, 171-185.
44. A. Charpentier, M. SimmonsMenchaca, W. P. Yu, B. H. Zhao, M. Qian, K. Heim, B. G. Sanders and K. Kline, *Nutr. Cancer*, 1996, **26**, 237-250.
45. M. Qian, B. G. Sanders and K. Kline, *Nutr. Cancer*, 1996, **25**, 9-26.
46. M. Fariss, M. Fortuna, C. Everett, J. Smith, D. Trent and Z. Djuric, *Cancer Res.*, 1994, **54**, 3346-3351.
47. J. M. Turley, F. W. Ruscetti, S.-J. Kim, T. Fu, F. V. Gou and M. C. Birchenall-Roberts, *Cancer Res.*, 1997, **57**, 2668-2675.
48. Y. W. Won, S. M. Yoon, K. S. Lim and Y. H. Kim, *Adv. Funct. Mater.*, 2012, **22**, 1199-1208.
49. Y. Tao, J. Han and H. Dou, *J. Mater. Chem.*, 2012, **22**, 8930-8937.
50. S. Hong, P. R. Leroueil, I. J. Majoros, B. G. Orr, J. R. Baker, Jr. and M. M. Banaszak Holl, *Chem. Biol.*, 2007, **14**, 107-115.
51. D. Cakara, J. Kleimann and M. Borkovec, *Macromolecules*, 2003, **36**, 4201-4207.
52. P. Garin-Chesa, I. Campbell, P. Saigo, J. Lewis Jr, L. Old and W. Rettig, *Am. J. Pathol.*, 1993, **142**, 557.

Table 1. Zeta potential values of G5.NHAc$_n$-α-Tos-FI and G5.NHAc$_n$-α-Tos-FI-FA conjugates under different pH conditions.

Materials	Zeta potential (mV)		
	pH = 5.0	pH = 7.0	pH = 10.0
G5.NHAc$_n$-α-Tos-FI	21.3 ± 1.1	10.2 ± 1.4	-15.5 ± 0.8
G5.NHAc$_n$-α-Tos-FI-FA	13.5 ± 1.0	5.5 ± 1.4	-2.4 ± 0.8

Figure captions

Scheme 1. Schematic illustration of the synthesis of G5.NHAc$_n$-α-Tos-FI-FA conjugate.

Figure 1. ^{1}H NMR spectrum of G5.NHAc$_n$-α-Tos-FI-FA conjugate.

Figure 2. UV-Vis spectra of α-Tos dissolved in ethanol, and G5.NH$_2$, G5.NH$_2$-α-Tos, G5.NHAc$_n$-α-Tos, G5.NHAc$_n$-α-Tos-FI, and G5.NHAc$_n$-α-Tos-FI-FA dendrimers or conjugates dissolved in aqueous solution.

Figure 3. MTT viability assay of KB cells after treatment with 10 μL PBS, 1 μL ethanol, free α-Tos (12.5, 25, 50, 100, 200 μM) in 1 μL ethanol, G5.NHAc$_n$-α-Tos-FI or G5.NHAc$_n$-α-Tos-FI-FA conjugate (with α-Tos concentration of 12.5, 25, 50, 100, and 200 μM, respectively) dissolved in 10 μL PBS, and G5.NHAc$_n$-FI-FA dendrimer (2.5, 5, 10, 20, and 40 μM, respectively) dissolved in 10 μL PBS. The data are expressed as mean ± S.D.

Figure 4. Confocal microscopic images of KB-HFAR cells incubated with PBS, KB-LFAR cells and KB-HFAR cells treated with G5.NHAc$_n$-α-Tos-FI and G5.NHAc$_n$-α-Tos-FI-FA conjugate (both with α-Tos concentration of 0.4 μM), respectively. All images were collected under similar instrumental conditions.

Figure 5. MTT viability assay of KB-HFAR and KB-LFAR cells after treatment with G5.NHAc$_n$-α-Tos-FI or G5.NHAc$_n$-α-Tos-FI-FA conjugates at the α-Tos concentration of 50 μM. The KB-HFAR cells treated with PBS and free α-Tos (1 μL ethanol, [α-Tos] = 50 μM) were used as control.

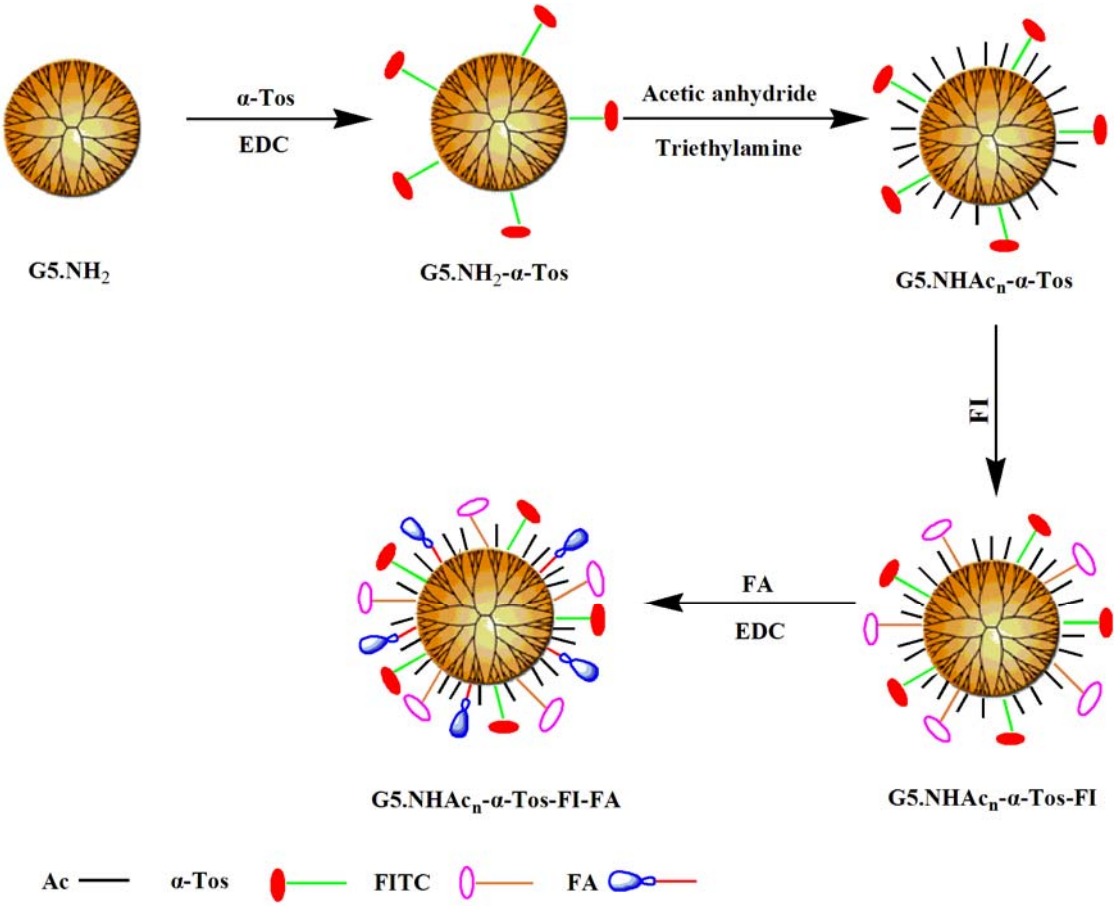

Scheme 1

Zheng et al.

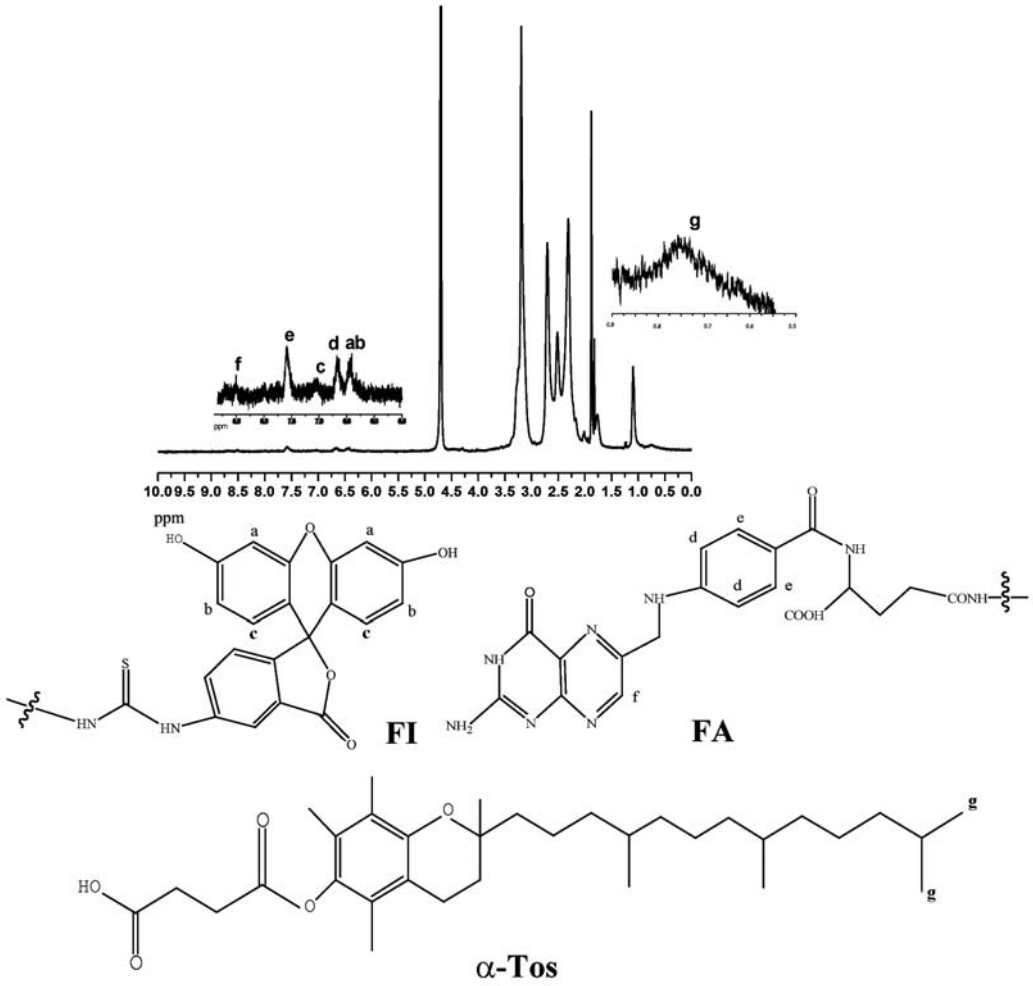

Figure 1

Zheng et al.

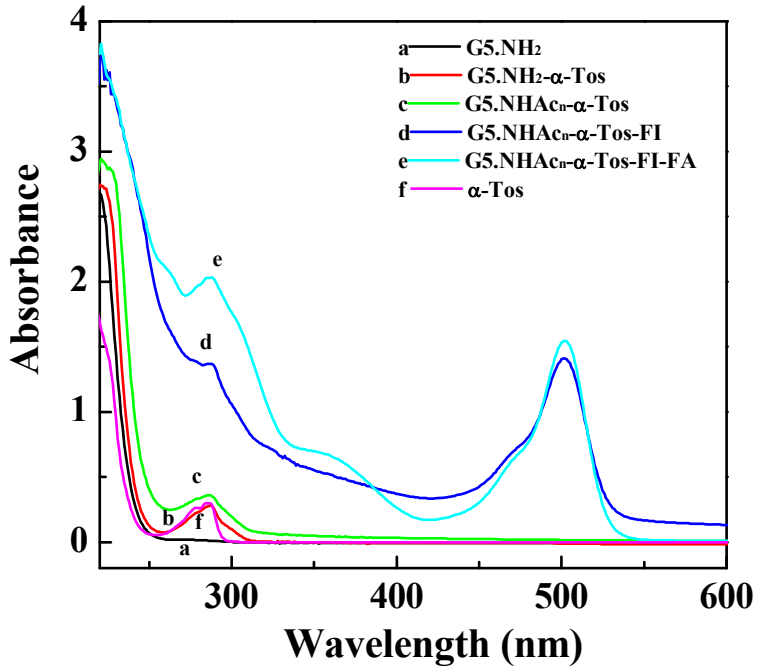

Figure 2

Zheng et al.

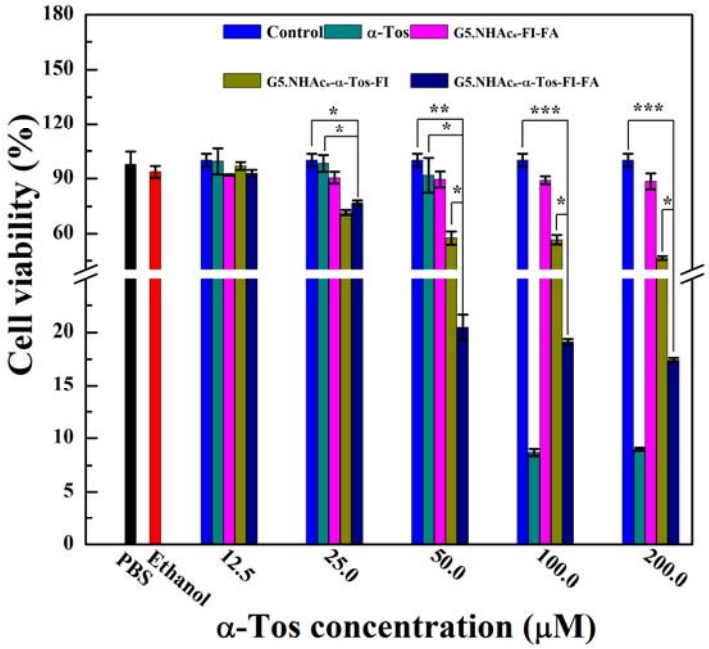

Figure 3

Zheng et al.

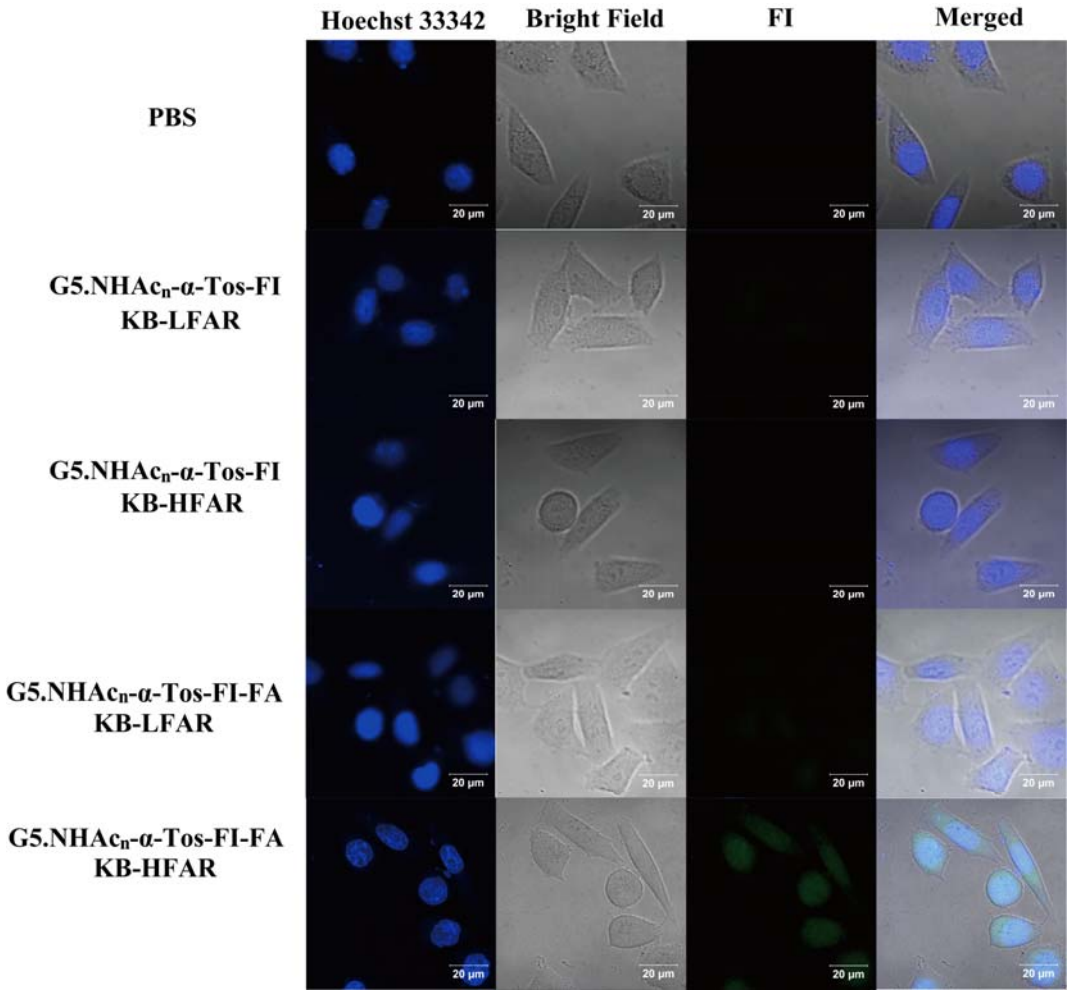

Figure 4

Zheng et al.

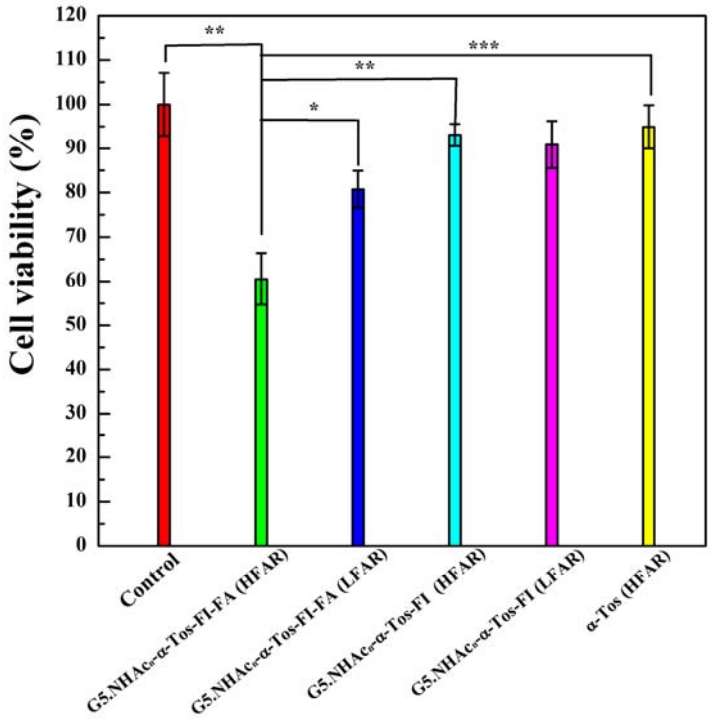

Figure 5

Zheng et al.